Clays and Clay Minerals, 1972, Vol. 20, pp. 303–315. Pergamon Press. Printed in Great Britain

THE OXIDATION OF OCTAHEDRAL IRON IN BIOTITE

R. J. GILKES, R. C. YOUNG and J. P. QUIRK
Department of Soil Science and Plant Nutrition, Institute of Agriculture,
University of Western Australia, Nedlands, Western Australia 6009

(*Received* 10 *April* 1972)

Abstract—Oxidation of octahedral ferrous iron in biotite by saturated bromine water results in a loss of both octahedral and interlayer cations. The hydroxyl adjacent to vacant octahedral cation sites adopt an inclined orientation resulting in a more stable environment for interlayer cations. The only structural change accompanying these processes is a decrease in *b*-axis dimension which is linearly related to octahedral ferric iron content. These findings are in agreement with observations made on naturally weathered biotites.

INTRODUCTION

BIOTITE is not often a major constituent of rocks although it is present in small quantities in many common igneous and metamorphic rock types. The importance of biotite as a source of plant nutrients is often far greater than would be predicted from the levels found in soil parent materials. This is a consequence of two important properties of the mineral; its resistance to alteration in comparison with most ferromagnesian minerals and the common occurrence of several essential micro- and macro-nutrient elements in interlayer and octahedrally coordinated sites. Jackson (1964) has shown that biotite will persist in soils under weathering conditions that alter other ferromagnesian minerals while Denison *et al.* (1929) have observed that oxidized biotite shows a marked resistance to alteration. In these situations biotite may become a major source of K, Mg, Zn, Mn and other elements to plants as it slowly alters to secondary minerals in the root zone. Biotite flakes isolated from soils and weathered rocks invariably contain more ferric iron than flakes separated from unaltered parent material. Sometimes the oxidation of octahedrally coordinated iron may be the only significant change that occurs during the early stages of biotite weathering. More usually broadening and minor displacement of reflections in X-ray diffraction patterns occur and losses of both interlayer and octahedrally coordinated ions take place (Walker, 1949). Eventually conversion to vermiculite or montmorillonite (Barshad, 1966) may occur but the initial loss of structural cations take place without major changes in crystal structure. The loss of octahedrally coordinated cations during weathering gives oxidized biotites an increasingly dioctahedral character. Some properties of oxidized biotites resemble those of dioctahedral micas with a correspondingly higher resistance to potassium removal and an increased potassium fixing capacity. This behaviour has been noted by Denison and Fry (1929) in their field studies of biotite weathering and in laboratory experiments by several workers (Barshad and Kishk, 1968; Dyakonov and L'vova, 1967; Robert and Pedro, 1969).

An understanding of changes that occur in the composition of biotites during oxidation is necessary if the factors controlling release of structural ions to soil solution are to be understood.

Published investigations of the properties of laboratory oxidized biotites have either involved chemical pretreatment to convert biotite to an expanded phase prior to or during oxidation (Ismail, 1969; Farmer and Wilson, 1970; Farmer *et al.*, 1971) or have used thermal treatments resulting in losses of hydroxyl (Robert and Pedro, 1969). Neither technique produces oxidized biotites resembling those found in soils, i.e. with a normal but broadened X-ray diffraction pattern and an almost unaltered hydroxyl content. This study describes the preparation and properties of oxidized biotites identical to those occurring in soils.

MATERIALS AND METHODS

Materials

The results described in this paper are for less than 10μ fraction of a biotite specimen from Bancroft, Ontario, supplied by Wards Natural Science Establishment, Inc., New York. Different particle size fractions of this biotite and of several Australian biotites were also used for some experiments. The results obtained for these specimens

https://doi.org/10.1346/CCMN.1972.0200507 Published online by Cambridge University Press

were substantially the same as those for less than 10μ Bancroft and are not described here.

Preparation of oxybiotite

A single 100 g sheet of biotite free of inclusions was cut into centimeter square flakes which were ground for 8 min in the agate vessel of a Tema disc mill. The less than 10 μ fraction was obtained by sedimentation after dispersion in water. Five gram portions of this material were immersed in 100 ml of saturated bromine solution in sealed glass ampoules. The ampoules were shaken in an end-over-end shaker at 90°C for 1, 2, 3, 5 and 14 days. Bromine was removed by gentle boiling and the biotite washed several times with distilled water before drying at 110°C.

Chemical analysis

Replicate 100 mg samples of biotite were dissolved in 2 ml of 40% HF and 2 ml of 70% $HClO_4$ in a 20 ml teflon crucible. The crucible was heated on a hotplate until fuming ceased when a further 2 ml of $HClO_4$ was added and heating continued until almost dry. After cooling 5 ml of distilled water and 5 ml of conc. HCl were added and the crucible heated until all the solid material has dissolved. The solution was then made up to 100 ml with 3000 ppm $SrCl_2$ prior to analysis by atomic absorption spectrometry. Some samples were also analysed by X-ray fluorescence spectrometry and by colorimetric techniques. Good agreement was found with atomic absorption results.

Ferrous iron was determined by titration against potassium dichromate using barium diphenylaminesulphonate indicator (in the presence of 10% H_2SO_4/10% H_3PO_4) after dissolution of the sample in HCl/HF under a CO_2 atmosphere.

Silicon was determined by atomic absorption spectrometry. Samples were dissolved in a $Na_2CO_3/Na_2B_4O_7$ fusion mixture and subsequently dissolved in 3M HCl.

Analyses were made of standard biotites VT194 (Institute of Mineralogy and Petrology, University of Basle) and Mica.Fe (Centre de Recherches Petrographiques et Géochimiques Université de Nancy) by these techniques and excellent agreement found with the reported values.

Dithionite extraction

Replicate 100 mg samples of biotite in 10 ml centrifuge tubes were shaken for 5 min with 8 ml 0·3M sodium citrate and 1 ml 1M $NaHCO_3$ at 80°C. 2 ml of 5% sodium dithionite were then added and the tubes shaken for a further 5 min. The suspension was then centrifuged and the supernatant removed. This process was repeated 5 times. 5 ml of conc. HNO_3 was added to the dithionite extracts which were then boiled until almost dry. 5 ml of conc. HCl was added and the solution heated until fuming ceased. The solution was then transferred into 25 ml flasks and made up to volume with 3000 ppm $SrCl_2$ solution prior to analysis by atomic absorption spectrometry.

X-ray diffraction

A Phillips vertical diffractometer with suitably filtered Co and Cu radiations was used. Precision measurements of changes in 2θ values of biotite (060) and (005) reflections were made using an automatic step scanning device which permitted the accumulation of 4000 counts at 0·02° intervals of 2θ. These measurements were each repeated 3 times and mean values obtained. The influence of goniometer temperature fluctuations on these measurements was minimized by operating in a controlled temperature (20° $\pm$ 2°C) environment and by relating peak positions to those of standards run immediately before and after the specimen. The full width at half height of the (003) biotite reflection was also measured by step scanning using a 0·05 mm receiving slit. The corresponding crystal thickness was derived from the Scherrer equation using an instrumental broadening factor obtained from a less than 2 μ quartz specimen which diffracts at the same Bragg angle. Diffraction patterns were also made of basally oriented biotite films on ceramic plates saturated with magnesium, glycerol and cetyl pyridinium bromide. These techniques provide a more sensitive means of detecting interlayers of vermiculite and montmorillonite than random powder mounts of micas.

Electron-optical techniques

Scanning electron microscope pictures were obtained with a Jeol S.E.M. 2 scanning microscope of aluminium coated less than 100 mesh biotite flakes. Transmission electron micrographs and electron diffraction patterns were made using a Hitachi HU11 microscope. Specimens were prepared by allowing a drop of very dilute suspension to dry on a carbon coated grid.

I.R. measurements

All i.r. spectra were recorded on a Perkin-Elmer 337 instrument. Samples were dispersed in KBr discs according to the method of Farmer *et al.* (1971). The discs were subsequently heated for 24 hr at 50°C temperature intervals to 600°C. Single flakes of biotite and basally oriented preparations in Nujol on silver chloride discs were also examined at various angles of incidence.

https://doi.org/10.1346/CCMN.1972.0200507 Published online by Cambridge University Press

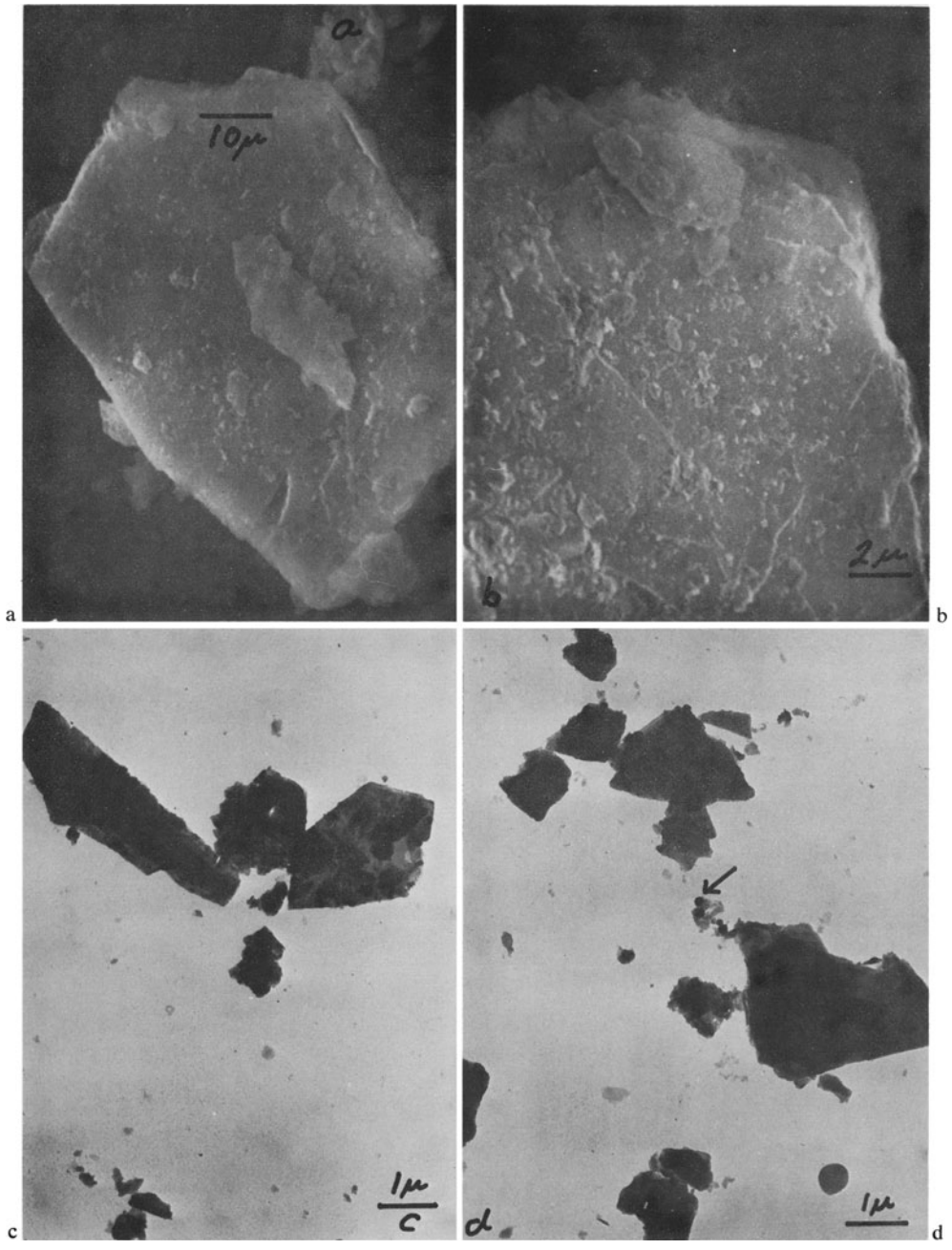


Fig. 1. (a) Scanning electron micrograph of < 100 mesh biotite before oxidation treatment. (b) Scanning electron micrograph of < 100 mesh biotite after eight days oxidation treatment. (c) Transmission electron micrograph of < 10 μ biotite before oxidation treatment. (d) Transmission electron micrograph of < 10 μ biotite after 14 days oxidation treatment.

[*Facing page* 304]

https://doi.org/10.1346/CCMN.1972.0200507 Published online by Cambridge University Press

RESULTS AND INTERPRETATION

Morphology and structure

Artificially oxidized biotites show the characteristic golden luster of naturally occurring specimens. The intensity of this luster increases with treatment time. Of all size fractions examined only the greater than 100 mesh material showed a non uniform color and then only at the initial stages of oxidation. The appearance of these flakes which have dark grey centers and golden rims indicates that an oxidation front moves in from the edge of the crystal in a similar manner to the K depletion front described by Raussel-Colom *et al.* (1965). Once the oxidation front reaches the center of crystal further oxidation increases the golden color uniformly throughout the crystal with thicker crystals developing a more intense color. Optical and electronoptical examination shows that there is little evidence of dissolution during oxidation. The small (less than 0·2 μ) electron dense clumps seen in Fig. 1d, which do not give electron diffraction patterns, may be iron oxides. The major physical effect of the oxidation treatment is to cleave small fragments off the crystals as shown by the scanning electron microscope pictures of less than 100 mesh biotite before and after oxidation in Figs. 1a–b and by transmission electron micrographs of the less than 10 μ fraction in Figs. 1c and d. The effect of oxidation on the particle size distribution of less than 100 mesh biotite is also shown by the sieve analysis in Table 1. A similar reduction in particle size of less than 10 μ fraction is evident in Figs. 1c and 1d. Measurements of average crystal thickness of oxidized, less than 10 μ biotite using X-ray diffraction line broadening data are shown in Fig. 2. This data indicates that the average crystal thickness of the most oxidized biotite is one third the average crystal thickness of the starting material. Values of particle size obtained by this technique are sensitive to the presence of interlayers of montmorillonite or vermiculite so that the thicknesses shown in Fig. 2 may underestimate the true values. The basal reflections are symmetrically broadened and do not vary in spacing by more than 0·2% (Fig. 3) so that little or no interlaying occurs.

The integrated intensity of biotite (060) and (005) reflections decreases by approx. 20% with increasing oxidation as shown in Table 2. This indicates that no major changes take place in the biotite structure and that little amorphous material is present. Changes in the occupation of octahedral sites as described below will also influence the intensity of these reflections. No reflection from iron oxides or other crystalline alteration products were found in X-ray diffraction patterns but since the electron dense clumps observed on the cleavage faces of oxidized biotite crystals are amorphous to electrons they would not be expected to diffract X-rays.

The unit cell dimensions of micaceous minerals vary with composition and several formulae have been proposed relating chemical composition to

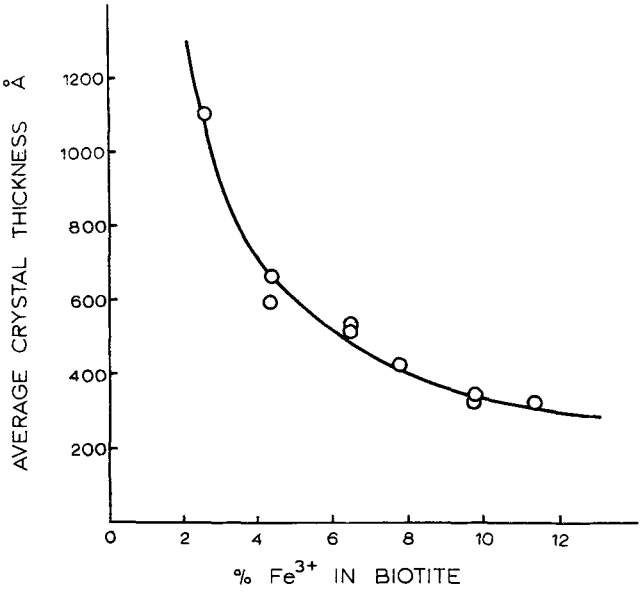


Fig. 2. Average crystal thickness of oxidized biotite crystals determined from line broadening of the (003) reflection.

https://doi.org/10.1346/CCMN.1972.0200507 Published online by Cambridge University Press

Table 1. Particle size distribution and ferrous iron content of oxidized biotite

	< 400 mesh	200–400 mesh	100–200 mesh
Original	51% (11·6% Fe^{2+})	18% (12·8% Fe^{2+})	31% (13·6% Fe^{2+})
Oxidized 10 days	56 (8·5)	18 (10·5)	26 (10·5)
Oxidized 25 days	63 (6·5)	17 (7·2)	20 (8·0)

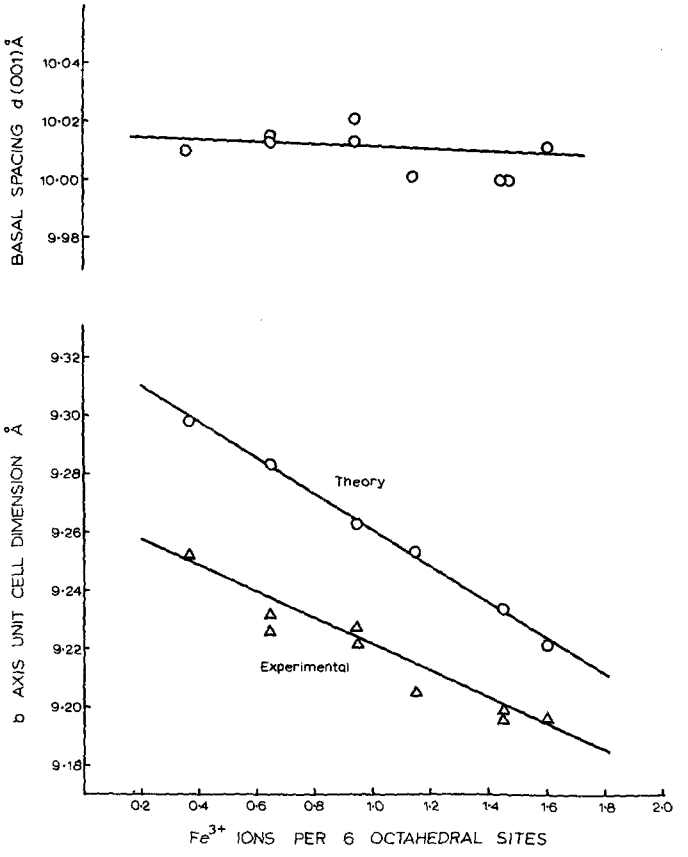


Fig. 3. Basal spacing $d(001)$ and b axis dimension of oxidized biotites as a function of ferric iron content.

unit cell parameters (Brindley and MacEwan, 1953; Radoslovich, 1962). Figure 3 shows the changes in $d(001)$ and b-axis unit cell dimension that occur during oxidation of biotite. There is no significant change in basal spacing and a linear decreases in b-axis spacing with increasing ferric iron content. Also shown in Fig. 3 is a line derived from points for each biotite calculated from the formula of Brindley and MacEwan (1953) relating b-axis spacing of micaceous minerals to chemical composition. The two graphs have similar slopes but are not coincident. This is probably due to errors in the absolute determination of lattice spacing in this work and the presence of vacant octahedral sites in this biotite which may influence the position of the theoretical curve (Brown, 1965). The similar slopes of the two graphs support the optical observation that oxidation occurs uniformly throughout the crystal and that zones of high and low ferric iron are not present. If this was not the case a composite (060) reflection would occur with components of different lattice spacing.

https://doi.org/10.1346/CCMN.1972.0200507 Published online by Cambridge University Press

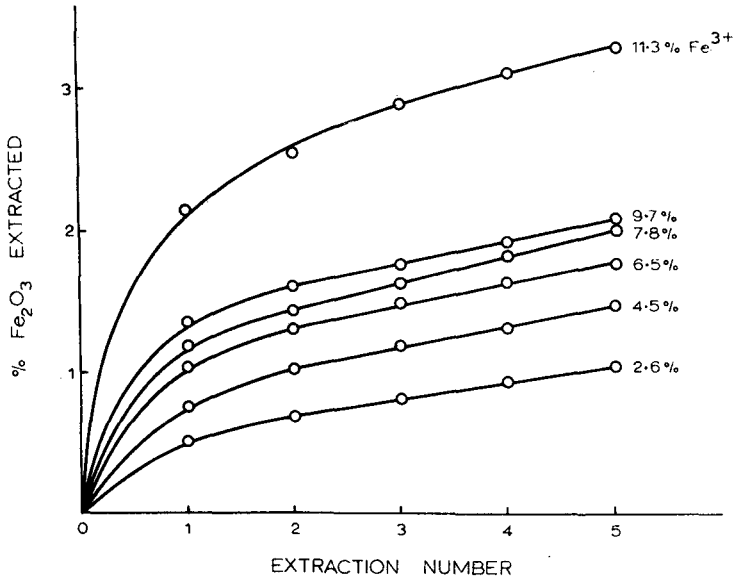


Fig. 4. Percentage Fe_2O_3 extracted from oxidized biotites by successive sodium dithionite treatments.

Table 2. Normalized integrated intensity of (005) and (060) reflections for oxidized biotite

	Normalized intensity (005)	(060)
Original	100	100
Day 1	101	87
Day 2	85	86
Day 3	80	79
Day 5	84	80
Day 14	73	88

Chemical composition

Chemical analyses of the series of less than 10 μ oxidized biotites including replicate 1, 2 and 5 day treatments are shown in Table 3. The replicates are in excellent agreement showing that this technique may be used to prepare specimens of any desired ferric iron content. Silicon is the only element to increase in concentration during oxidation. It does so at the expense of other structural cations particularly those in octahedral and interlayer sites. Total iron remains constant but this may be due to the precipitation of amorphous oxides on the surface of biotite flakes. The trends in composition closely resemble the results obtained on naturally oxidized biotites by Walker (1949) and Robert and Pedro (1969). Calculation of structural formulae from these analyses requires an estimate of the proportion of iron, silicon, and other elements that are not present in structural sites in biotite but as surface coatings and amorphous residues. Farmer *et al.* (1971) found lath-like crystals of microcrystalline β-FeOOH (akaganéite) on the surface of bromine oxidized, barium saturated vermiculites. Similar crystals were seen in this study on barium chloride/bromine treated biotites but were not observed for water/bromine treated biotites. In the water/bromine oxidized biotites only the small electron dense clusters shown in Fig. 1d were seen, which are probably a form of amorphous iron oxide. The amount of surface iron oxides may be estimated by successive dithionite extractions as described by Farmer *et al.* (1971). After a large loss in the first extraction, subsequent extractions remove iron at an almost constant rate due to dissolution of biotite (Fig. 4). This indicates that the amount of surface iron may be estimated by extrapolation of these curves back to the ordinate. The amount of surface iron released shows an approximately linear relation with the initial ferric iron content (Fig. 5) supporting the concept that iron and other octahedral cations are ejected to preserve electrical neutrality.

Confirmation that dissolution of oxidized biotites is taking place at an approximately constant rate during dithionite treatment is given by the curves for magnesium lost during dithionite extraction (Fig. 6). Only the original biotite shows a large initial loss of magnesium. This is probably easily released surface magnesium that had been removed

https://doi.org/10.1346/CCMN.1972.0200507 Published online by Cambridge University Press

Table 3. Chemical analyses (per cent) of oxidized biotites and standard biotites VT194 and mica–Fe

	Original	Day 1a	Day 1b	Day 2a	Day 2b	Day 3	Day 5a	Day 5b	Day 14	VT194	VT194*	Mica Fe	Mica Fe†
SiO_2	38·4	39·1	—	40·0	—	40·1	39·0	—	40·2	37·7	37·4	35·6	34·4
TiO_2	2·3	—	—	—	—	—	—	—	—	—	2·5	—	—
Al_2O_3	11·7	11·8	—	11·3	—	11·5	11·5	—	11·1	17·6	17·7	19·5	19·4
Fe_2O_3	3·71	6·38	6·35	9·35	9·45	11·18	13·89	14·1	16·18	1·84	1·6	3·95	3·60
FeO	15·37	12·97	13·0	10·31	10·20	8·69	6·23	6·01	4·35	10·6	10·6	19·8	19·8
MnO	1·00	0·95	0·95	0·92	0·94	0·92	0·86	0·86	0·79	0·09	0·1	0·38	0·37
ZnO	0·085	0·081	0·080	0·075	0·074	0·073	0·069	0·066	0·063	—	—	—	—
MgO	13·3	12·8	12·8	12·6	12·6	12·3	12·2	12·2	11·8	16·4	16·3	5·1	4·55
CaO	0·16	—	—	—	—	—	—	—	—	—	0·1	—	0·50
Li_2O	0·111	0·104	—	0·101	—	0·098	0·092	—	0·088	—	—	—	—
Na_2O	0·49	0·42	0·43	0·39	0·38	0·37	0·28	0·31	0·28	—	0·04	—	0·25
K_2O	9·13	8·34	8·29	8·14	8·20	7·96	7·89	7·95	7·64	9·06	9·10	8·80	8·80
F	2·30	—	—	—	—	—	—	—	—	—	—	—	—
H_2O^+	1·1	—	—	—	—	—	—	—	—	—	—	—	—

*University of Basle.
†Centre de Recherche Petrographiques et Geochimiques de Nancy.

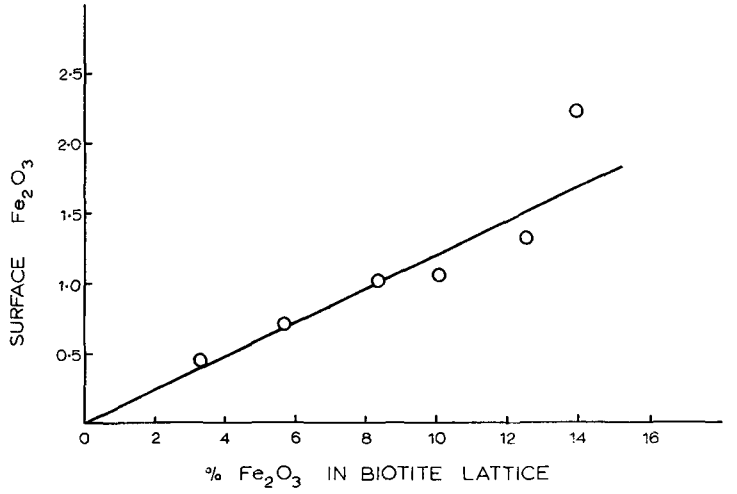


Fig. 5. Surface Fe_2O_3 on oxidized biotite as a function of structural Fe_2O_3 in biotite.

during oxidation treatment of the other specimens. If the curve for the original biotite is corrected for this initial loss and all the curves plotted as the percentage of total magnesium lost against extraction number they approximately coincide. This indicates that the rate of dissolution of biotite in a reducing environment is not sensitive to the initial oxidation state of octahedral iron. This is not the case in a mildly oxidizing environment where experiments in artificial weathering of oxidized biotites have shown that specimens with high ferric iron contents are more stable than the corresponding ferrous biotites. These results, which will be described in a later publication, show that the commonly accepted theory that oxidation of octahedral ferrous iron accelerates biotite decomposition is in fact incorrect (Arnold, 1960).

Silicon-rich fringes have been observed (Gastuche, 1963) surrounding acid treated biotite crystals and would contribute to the increased silicon content if these are present in these samples. No such fringes were observed using high resolution dark and bright field electron microscopy so that even if very thin fringes are present they do not contribute significantly to the increased silicon content. A further difficulty encountered in the calculation of structural formulae for oxidized biotites is in determining the composition of the

https://doi.org/10.1346/CCMN.1972.0200507 Published online by Cambridge University Press

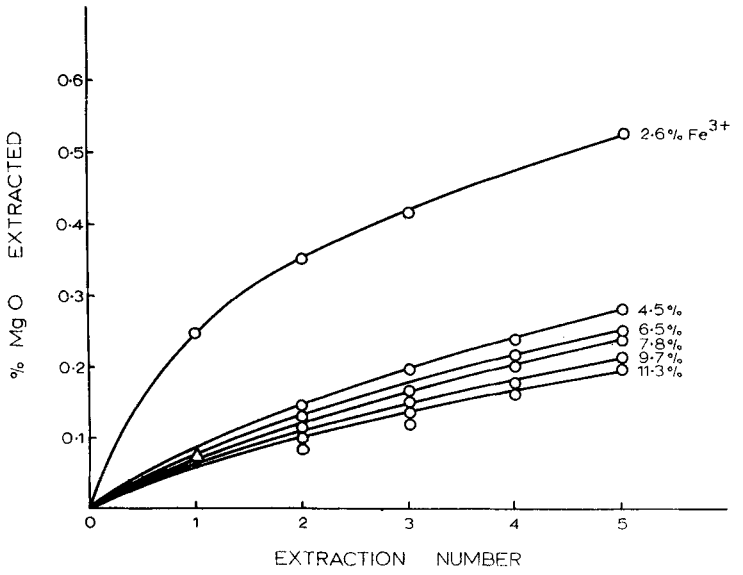


Fig. 6. Percentage MgO extracted from oxidized biotite by successive sodium dithionite treatments.

anion framework (Rimsaite, 1970). It was not possible to resolve the various types of structural OH and adsorbed water by ignition techniques since all are lost over wide and overlapping temperature ranges and hydrogen may also be lost. Insufficient sample was available to determine the anion composition of the oxidized biotites so that structural formulae (Table 4a) were calculated on the basis of a constant anion framework of 44 negative charges per unit cell contents (Foster, 1960). This assumption introduces an increasingly large error in the distribution of cations in the various sites if significant changes in anion composition occur during oxidation (Rimsaite, 1970). The series of structural formulae derived in this way are internally consistent in that they show no movement of cations between structural sites during oxidation and a progressive loss of interlayer and octahedrally coordinated ions. The total occupancy of tetrahedral sites remains almost constant with only a minor change in silicon to aluminium ratio. This is consistent with the high stability shown by silicon–oxygen tetrahedra in layer silicates during weathering and contrasts with the rapid loss of octahedrally coordinated and interlayer cations. Several workers have noted a similar change in the tetrahedral composition of soil illites derived by the weathering of micas (Arnold, 1960; Walker, 1949). The increase in dioctahedral character due to ejection of octahedral cations is also shown by naturally occurring weathered biotites (Walker, 1949; Robert and Pedro, 1969) and vermiculites (Wilson, 1970). The quantity of surface iron oxides estimated by dithionite extraction may be subtracted from the total ferric iron and structural formulae calculated on an oxide free basis. These formulae (Table 4b) differ from those including dithionite extractable iron (Table 4a) in having a higher occupancy of tetrahedral sites and a lower occupancy of octahedral sites particularly by ferric iron.

Both sets of structural formulae demonstrate that charge balance in oxidized biotites is achieved by loss of interlayer and octahedral cations with little change in the tetrahedral layer and micaceous structure. This is not the case with thermally oxidized biotites which retain a 10 Å basal spacing and release only protons to preserve neutrality. Bromine oxidized vermiculites were described by Farmer *et al.* (1971) in which a similar loss of iron was observed. The common occurrence of iron oxides on the surface of weathered biotite flakes (Wilson, 1970) and the observations of Farmer *et al.* (1971) on both naturally occurring and bromine oxidized vermiculites and hydrobiotites indicate that the structural formulae in Table 4b are probably more appropriate than those in Table 4a. Thus iron is ejected along with other octahedral cations and at a similar rate to magnesium. Manganese and zinc are lost at a faster rate, an observation which has been confirmed by similar experiments using other biotite specimens, although no satisfactory explanation for this behaviour is known. Similarly, sodium is released from inter-

https://doi.org/10.1346/CCMN.1972.0200507 Published online by Cambridge University Press

Table 4. Structural formulae for oxidized biotites calculated on the basis of 44 charges

	Original	Day 1	Day 2	Day 3	Day 5	Day 14
(a). *Including dithionite soluble iron*						
Si	5·83 } 7·93	5·88 } 7·97	5·95 } 7·93	5·93 } 7·94	5·85 } 7·85	5·93 } 7·86
Al	2·10	2·09	1·98	2·01	2·00	1·93
Ti	0·24	0·24	0·23	0·23	0·23	0·23
Fe^{3+}	0·43	0·72	1·05	1·25	1·57	1·81
Fe^{2+}	1·93	1·63	1·28	1·08	0·78	0·55
Mn	0·13 } 5·79	0·12 } 5·65	0·12 } 5·55	0·12 } 5·47	0·11 } 5·48	0·10 } 5·35
Mg	2·98	2·87	2·80	2·72	2·73	2·60
Zn	0·01	0·01	0·01	0·01	0·01	0·01
Li	0·07	0·06	0·06	0·06	0·05	0·05
Ca	0·02	0·02	0·02	0·02	0·02	0·02
Na	0·14 } 1·93	0·13 } 1·76	0·11 } 1·68	0·11 } 1·64	0·09 } 1·63	0·08 } 1·56
K	1·77	1·61	1·55	1·51	1·52	1·46
Tetrahedral Charge	2·38	2·21	2·26	2·25	2·60	2·48
Layer Charge	1·95	1·78	1·70	1·66	1·65	1·58
(b). *Omitting dithionite soluble iron*						
Si	5·85 } 7·96	5·91 } 8·00	6·00 } 7·99	5·98 } 8·00	5·91 } 7·95	6·05 } 8·00
Al	2·11	2·09	1·99	2·02	2·04	1·95
Ti	0·24	0·24	0·23	0·23	0·23	0·23
Fe^{3+}	0·38	0·65	0·95	1·14	1·44	1·59
Fe^{2+}	1·94	1·64	1·29	1·09	0·78	0·56
Mn	0·13 } 5·77	0·12 } 5·61	0·12 } 5·48	0·12 } 5·39	0·11 } 5·37	0·10 } 5·17
Mg	3·00	2·89	2·82	2·74	2·75	2·64
Zn	0·01	0·01	0·01	0·01	0·01	0·01
Li	0·07	0·06	0·06	0·06	0·05	0·05
Ca	0·02	0·02	0·02	0·02	0·02	0·02
Na	0·14 } 1·94	0·13 } 1·76	0·11 } 1·69	0·11 } 1·65	0·09 } 1·64	0·08 } 1·56
K	1·78	1·61	1·56	1·52	1·53	1·46
Tetrahedral Charge	2·27	2·09	2·03	2·02	2·24	1·95
Layer Charge	1·96	1·78	1·71	1·67	1·66	1·58

layer sites at a faster rate than potassium which may be subject to increased fixation by oxidized biotite (Barshad and Kishk, 1968). The most highly oxidized biotite in this series has only 5·17 ions in six octahedral sites indicating that it should exhibit properties intermediate between those of trioctahedral and dioctahedral micas. This has been confirmed by i.r. absorption measurements described below and studies of potassium release to sodium chloride and sodium tetra-phenyl boron solutions (Gilkes, Young and Quirk, 1972).

I.R. measurements

Measurement of i.r. absorption were restricted to the 1200–4000 cm^{-1} frequency range which includes hydroxyl absorption between 3500 and 3700 cm^{-1}. Biotites usually show several peaks in this region dependent on the population of the octahedral cation sheet. Assignments of each peak to a hydroxyl in coordination with a particular group of three octahedral cations or vacancies have been proposed by Farmer, Russell and Ahlrichs (1968) and Vedder (1964). Bancroft biotite shows two absorption bands centered at 3530 and 3660 cm^{-1} (Fig. 7). These are the low frequency (L.F.) and high frequency (H.F.) bands described by Rouxhet (1970) for biotite from this locality who considers the H.F. band to be due to hydroxyl associated with three octahedral cations and the L.F. band to be due to hydroxyl associated with two cations and a vacant octahedral cation site. The absorption at the H.F. band by single biotite flakes or oriented preparations increases when they are inclined to the beam, whereas the L.F. band decreases in intensity (Fig. 8). This is consistent with different orientations of hydroxyl

https://doi.org/10.1346/CCMN.1972.0200507 Published online by Cambridge University Press

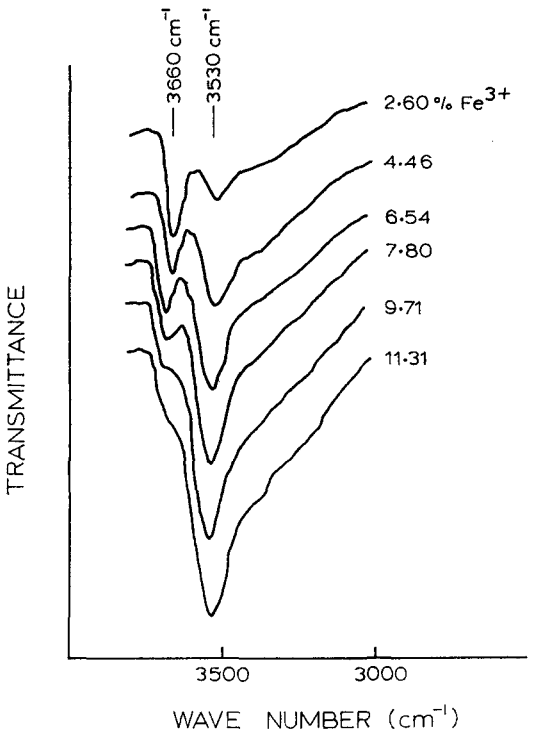


Fig. 7. I.R. absorption due to hydroxyl in oxidized biotites. Specimens prepared in KBr discs heated to 350°C.

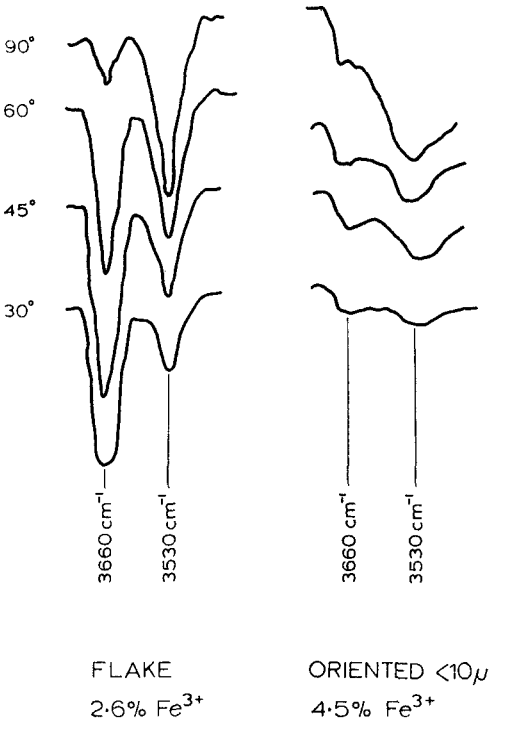


Fig. 8. I.R. absorption due to hydroxyl in biotite at various angles of incidence of the i.r. beam. Specimens are an unoxidized flake and an oriented sheet of partially oxidized biotite in Nujol on a silver chloride disc.

associated with filled and vacant octahedral cation sites (Serratosa and Bradley, 1958). Juo and White (1969) consider the L.F. band in oxidized biotite arises simply from the presence of octahedral ferric iron, whereas Farmer *et al.* (1971) assign the 3540 cm^{-1} peak to hydroxyl associated with a vacancy and a ferrous/ferric pair. These hydroxyl are in a similar configuration to those in nontronite which has a vacant site and two ferric ions per 3 octahedral sites and gives a broad peak centered at 3560 cm^{-1} (Farmer and Russell, 1964). The intensity of the L.F. peak increases for oxidized Bancroft biotite with an accompanying decrease in the intensity of the H.F. peak (Fig. 7). The abundance of hydroxyls contributing to the L.F. peak is linearly related to the ferric iron content of the biotite as shown by the linear relation between log transmittance at 3530 cm^{-1} and ferric iron (Fig. 9). The decrease in abundance of hydroxyls giving rise to the H.F. band also shows an approximately linear relation with ferric iron content. These results and the chemical data support the conclusion of Farmer *et al.* (1971) that, if the L.F. band is due to hydroxyl associated with vacancies, then vacancies are developed through the ejection of octahedral cations during oxidation. A linear relation between the abundance of vacancies and total ferric iron content, which includes surface iron, is also predicted by the calculated structural formulae as shown in Fig. 10. Similarly the decrease in number of filled sites in the structural formulae is linearly related to the abundance of 3660 cm^{-1} hydroxyl (Fig. 11). I.R. absorbance measurements show that the most highly oxidized biotite experiences a ninefold increase in vacancies in comparison with untreated biotite. This corresponds to a 4·3-fold increase in ferric iron showing that in the untreated biotite there are fewer vacancies that would be predicted from the initial ferric iron content alone. This is due to a higher octahedral cation population than is required to provide 12 units of positive octahedral charge for an ideal mica and the presence of other octahedral ions with charges less than the ideal 2 units. The extent of octahedral cation ordering may also influence the probability of a hydroxyl being associated with one or more vacant octahedral cation sites. The different slopes of the two lines in Fig. 9 show that there is not a one for one correspondence between the decrease in filled sites and increase in vacant sites. This may be partly due to differences in the absolute

https://doi.org/10.1346/CCMN.1972.0200507 Published online by Cambridge University Press

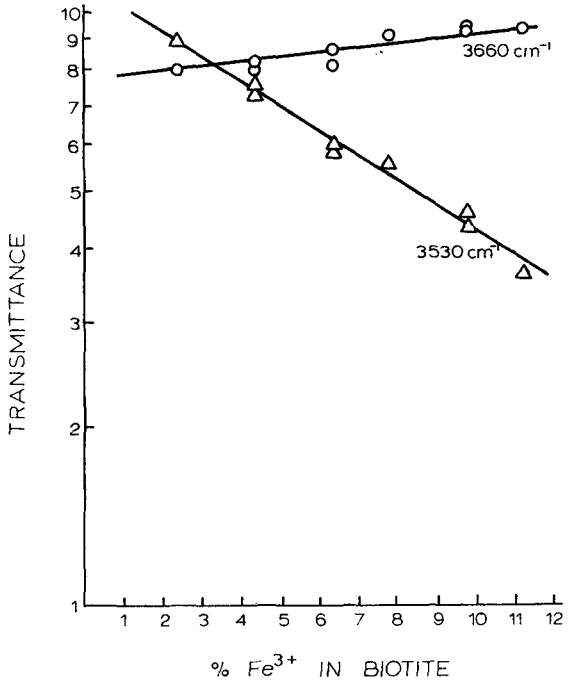


Fig. 9. Logarithm of transmittance at L.F. and H.F. bands of oxidized biotite as a function of ferric iron content.

absorbance per hydroxyl in the two sites. Rouxhet (1970) found similar variations in his studies of the integrated absorbances of hydroxyl in different micas.

All the biotite specimens show a weak absorption peak at 1630 cm^{-1} due to water which persists with reduced intensity after heating at 500°C for 24 hr showing that it is not present as a surface sorbed layer. The L.F. and H.F. hydroxyl absorption bands and the 1630 cm^{-1} water peak decrease in intensity on heating at a similar rate, as shown in Fig. 12. This is contrary to the behaviour of celadonite (Farmer, Russell and Ahlrichs, 1968) in which hydroxyl associated with Fe^{3+} Fe^{3+} and Fe^{3+} Mg pairs are destroyed at lower temperatures than those associated with Fe^{2+} Al and Mg Al pairs which remain intact. However, a weak residual 3660 cm^{-1} peak remains after the 3530 cm^{-1} band has been completely removed by heating at 575°C for 24 hr showing that the filled site hydroxyl is slightly more stable than vacancy hydroxyl. Biotite specimens heated at temperature up to 500°C before incorporation into a KBr disc show identical behaviour to those heated in KBr discs, confirming that the dehydration of biotites may be studied by this method with no interference from KBr (Farmer, Russell and Ahlrichs, 1968). The location of water molecules giving rise to the 1630 cm^{-1} peak is unknown although illites frequently contain inter-

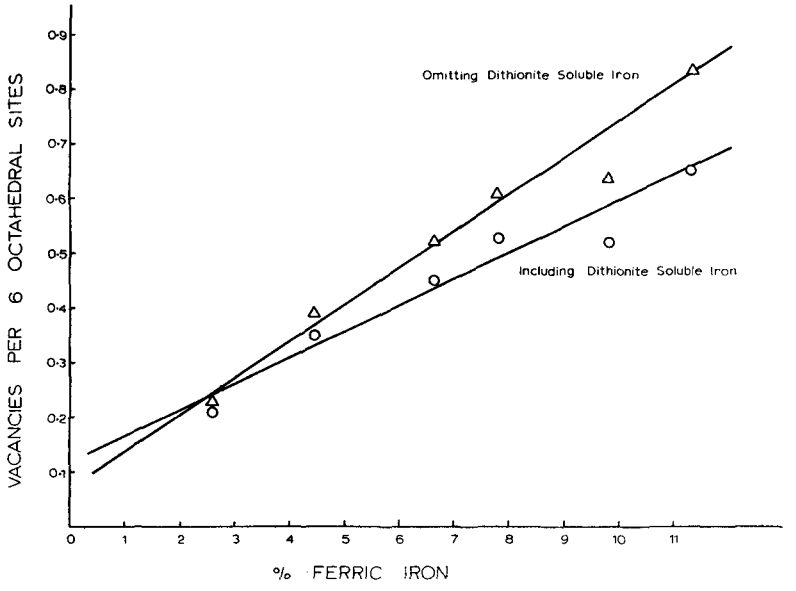


Fig. 10. The number of vacant octahedral cation sites (predicted by structural formulae in Table 4) as a function of the ferric iron content of oxidized biotite.

https://doi.org/10.1346/CCMN.1972.0200507 Published online by Cambridge University Press

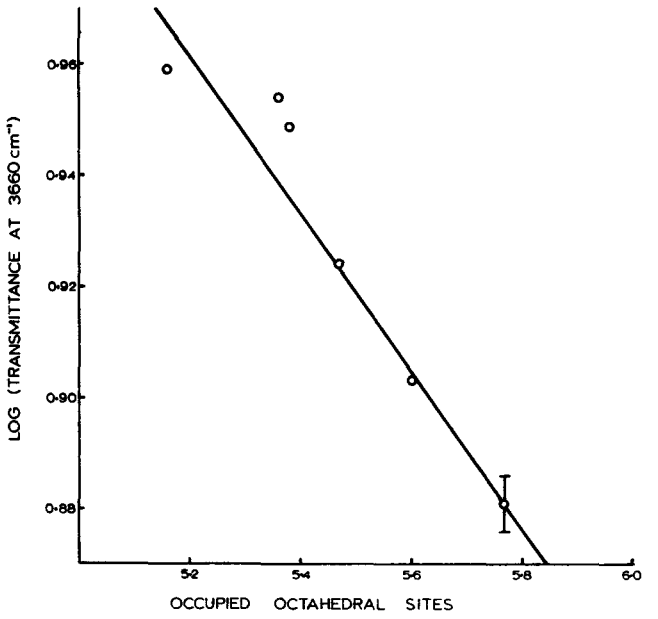


Fig. 11. Logarithm of transmittance at 3660 cm^{-1}, where absorption is due to hydroxyl associated with three filled octahedral cation sites, as a function of the number of such sites predicted by structural formulae in Table 4.

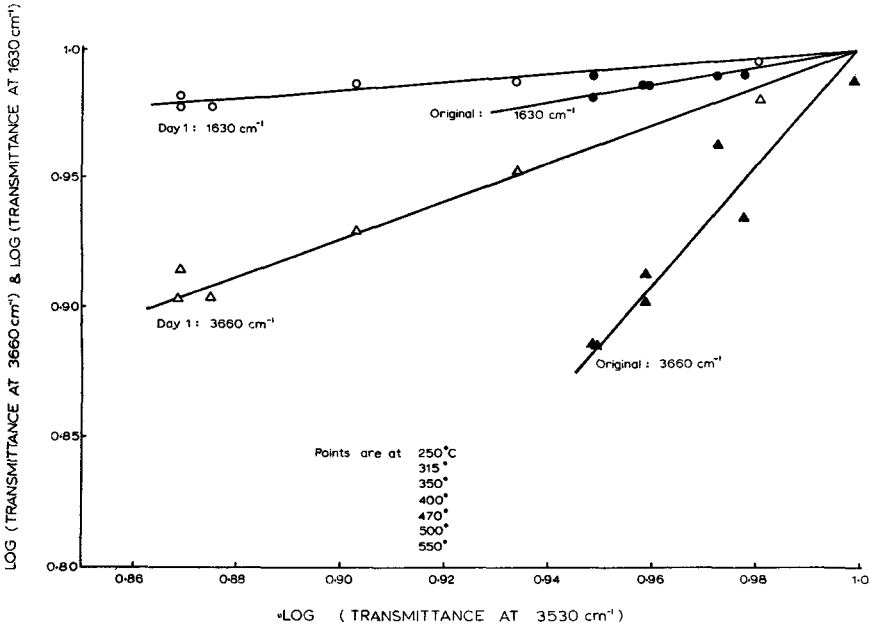


Fig. 12. Logarithms of transmittance at 3660 and 1630 cm^{-1} as a function of the logarithm of transmittance at 3530 cm^{-1} for biotite specimens heated at approximately 50°C temperature intervals up to 550°C.

https://doi.org/10.1346/CCMN.1972.0200507 Published online by Cambridge University Press

layer water which may occupy vacant potassium sites.

At attempt to reduce octahedral iron in oxidized biotite with hydrazine was unsuccessful and resulted in only a minor decrease in the intensity of the L.F. band and a minor increase in the intensity of the H.F. band. These results show that, unlike the findings of Farmer *et al.* (1971) for vermiculite, reduction of ferric iron does not occur and the generation of vacancies in biotite is not reversed by hydrazine treatment.

CONCLUSIONS

Oxidized biotite prepared by bromine oxidation is indistinguishable from naturally occurring specimens and may be used to investigate changes in chemistry and structure that occur during natural weathering. Because of its excellent reproducibility this technique produces specimens of any desired ferric iron content from an initially ferrous biotite.

The linear decrease in *b*-axis dimension with increasing ferric iron content is consistent with the behaviour predicted by theoretical studies. The increase in silicon content of the tetrahedral layer is characteristic of weathered micaceous minerals. Similarly, ejection of all species of interlayer and octahedral cation to preserve electrical neutrality is identical to the behaviour of naturally weathered biotites. The resultant change in orientation of vacancy hydroxyl decreases the repulsion of interlayer potassium, thereby increasing the minerals resistance to alteration. Since biotite is an important source of both major and micronutrients in some soils, the oxidation status of the mineral will influence the availability of these nutrients to plants.

Treatment of oxidized biotite with hydrazine does not reduce octahedral ferric iron or change the number of vacancy hydroxyl.

REFERENCES

Arnold, P. W. (1960) Nature and mode of weathering of soil-potassium reserves: *J. Sci. Food Agric.* **11**, 285–292.

Barshad, I. (1966) The effect of the variation in precipitation on the nature of clay mineral formation in soils of acid and basic igneous rocks: *Proc. Internat. Clay Conf.*, Jerusalem, Israel.

Barshad, I. and Kishk, F. M. (1968) Oxidation of ferrous iron in vermiculite and biotite alters fixation and replaceability of potassium: *Science* **162**, 1401–1402.

Brindley, G. W. and MacEwan, D. M. C. (1953) Structural aspects of the mineralogy of clays: *Ceramics—A Symposium*, pp. 15–59, The British Ceramic Society, Stoke-on-Trent.

Brown, G. (1965) Significance of recent structure determinations of layer silicates for clay studies: *Clay Miner.* **6**, 73–83.

Denison, I. A., Fry, W. H. and Gile, P. L. *Tech. Bull. U.S. Dep. Agric.* (1929) No. 128.

Dyakonov, Yu. S. and L'Vova, I. A. (1967) Transformation of trioctahedral micas into vermiculite: *Doklady Akad. Nauk. SSSR* **175**, 432–434.

Farmer, V. C. and Russell, J. D. (1964) The i.r. spectra of layer silicates. *Spectrochim. Acta* **20**, 1149–1173.

Farmer, V. C., Russell, J. D. and Ahlrichs, J. L. (1968) Spectroscopy of clay minerals: *Trans. 9th Int. Congr. Soil Sci. Adelaide, Australia* **3**, 101–110.

Farmer, V. C. and Wilson, M. J. (1970) Experimental Conversion of biotite to hydrobiotite: *Nature* **226**, 841–842.

Farmer, V. C., Russell, J. D., McHardy, W. J., Newman, A. C. D., Ahlrichs, J. L. and Rimsaite, J. Y. H. (1971) Evidence for loss of protons and octahedral iron from oxidised biotites and vermiculites: *Miner. Mag.* **38**, 121–137.

Foster, M. D. (1960) *Interpretation of the composition of trioctahedral micas*: *U.S. Geol. Surv. Profess. Paper* 354-B.

Gastuche, M. C. (1963) Kinetics of acid dissolution of biotite: *Proc. Int. Clay Conf. Stockholm* 67–83.

Gilkes, R. J., Young, R. C. and Quirk, J. P. (1972) Oxidation of ferrous iron in biotite: *Nature* **236**, 89–91.

Ismail, F. T. (1969) Role of ferrous iron oxidation in the alteration of biotite: *Am. Mineralogist* **54**, 1460–1466.

Jackson, M. L. (1964) Chemical composition of soils: In *Chemistry of the Soil* (Edited by Bear, F. E.), Reinhold, New York.

Juo, A. S. R. and White, J. L. (1969) Orientation of the dipole moments of hydroxyl groups in oxidised and unoxidised biotite: *Science* **165**, 804–805.

Radaslovich, E. W. (1962) The cell dimensions and symmetry of layer lattice silicates: *Am. Mineralogist* **47**, 617–636.

Raussel-Colom, J. A., Sweatman, T. R., Wells, C. B. and Norrish, K. (1965) In *Experimental Pedology* (Edited by Hallsworth, E. G. and Crawford, D. V.), Butterworth, London.

Rimsaite, J. (1970) Structural formulae of oxidised and hydroxyl-deficient micas and decomposition of the hydroxyl group: *Contr. Min. Petrol.* **25**, 225–240.

Robert, M. and Pedro, G. (1969) Etude des relations entre les phenomenes d'oxydation et l'aptitude à l'ouverture dans les micas trioctaedriques: *Proc. Int. Clay Conf. Japan.*

Rouxhet, P. G. (1970) Hydroxyl stretching bands in micas: a quantitative interpretation: *Clay Miner.* **8**, 375–388.

Serratosa, J. M. and Bradley, W. F. (1958) I.R. absorption of OH bonds in micas: *Nature* **181**, 111–112.

Vedder, W. (1964) Correlations between i.r. spectrum and chemical composition of mica: *Am. Mineralogist* **49**, 736–768.

Walker, G. F. (1949) The decomposition of biotite in the soil: *Miner. Mag.* **28**, 693–703.

Résumé—L'oxydation du fer ferreux octaédrique de la biotite par l'eau de brome saturée entraîne à la fois une perte de cations octaédriques et interfeuillets. L'hydroxyle adjacent au site cationique octaéd-

https://doi.org/10.1346/CCMN.1972.0200507 Published online by Cambridge University Press

rique vacant adopte une orientation inclinée entraînant un environnement plus stable pour les cations interfeuillets. Le seul changement de structure qui accompagne ces phénomènes est une diminution du paramètre *b* qui est relié linéairement à la teneur en fer ferrique octaédrique. Ces observations sont en accord avec celles que l'on peut faire sur les biotites altérées naturellement.

Kurzreferat — Die Oxydation von oktaedrischem Ferro-Eisen in Biotit durch gesättigtes Bromwasser ergibt einen Verlust an oktaedrischen sowie zwischenschichtigen Kationen. Die, freien oktaedrischen Kationenstellen benachbarten, Hydroxyle nehmen eine geneigte Richtung ein wodurch sich eine stabilere Umgebung für Zwischenschichtkationen ergibt. Der einzige, diese Vorgänge begleitende, Gefügewechsel ist eine Abnahme der *b*-Achsendimension, die in linearer Beziehung zu dem oktaedrischen Ferri-Eisengehalt steht. Diese Befunde stimmen überein mit Beobachtungen, die an natürlich verwitterten Biotiten gemacht wurden.

Резюме — Окисление октаэдрического железистого иона в биотите посредством насыщенной бромом водой, ведет к потере как октаэдрических так и межслоевых катионов. Гидроксил рядом с незаполненными октаэдрическими местонахождениями катионов принимают наклонную ориентацию в результате чего получается более стабильная среда для прослоечных катионов. Единственное структурное изменение сопровождающее эти процессы является уменьшение размера оси-b, линейно связанной с октаэдрическим содержанием железа. Эти данные совпадают с наблюдениями над естественно выветренными биотитами.

https://doi.org/10.1346/CCMN.1972.0200507 Published online by Cambridge University Press